

MECHANICAL PROPERTIES OF $\text{Ce}_{0.9}\text{Gd}_{0.1}\text{O}_{2-x}$ and $\text{Ce}_{0.9}\text{Gd}_{0.1}\text{O}_{2-x} + \text{Al}_2\text{O}_3$ COMPOSITES*

J. L. Routbort and K. C. Goretta
Energy Technology Division
Argonne National Laboratory, Argonne, IL 60439

R. Doshi, V. L. Richards, and M. Krumpelt
Chemical Technology Division
Argonne National Laboratory, Argonne, IL 60439

J. Wolfenstine
Division of Engineering
University of Texas at San Antonio, San Antonio, TX 72849

and A. R. de Arellano-López
Department of Condensed Matter Physics
University of Sevilla, Sevilla, Spain

RECEIVED
SEP 16 1999
OSTI

December 1997

The submitted manuscript has been created by the University of Chicago as Operator of Argonne National Laboratory ("Argonne") under Contract No. W-31-109-ENG-38 with the U.S. Department of Energy. The U.S. Government retains for itself, and others acting on its behalf, a paid-up, nonexclusive, irrevocable worldwide license in said article to reproduce, prepare derivative works, distribute copies to the public, and perform publicly and display publicly, by or on behalf of the Government.

Manuscript to be submitted to 22nd Annual Cocoa Beach Conference and Exposition of the American Ceramic Society, Cocoa Beach, January 20-24, 1998

*Work supported by the U.S. Department of Energy under Contract W-31-109-Eng-38; and the Ministerio de Educación y Ciencias, under CICYT Project MAT94-0481.

DISCLAIMER

This report was prepared as an account of work sponsored by an agency of the United States Government. Neither the United States Government nor any agency thereof, nor any of their employees, make any warranty, express or implied, or assumes any legal liability or responsibility for the accuracy, completeness, or usefulness of any information, apparatus, product, or process disclosed, or represents that its use would not infringe privately owned rights. Reference herein to any specific commercial product, process, or service by trade name, trademark, manufacturer, or otherwise does not necessarily constitute or imply its endorsement, recommendation, or favoring by the United States Government or any agency thereof. The views and opinions of authors expressed herein do not necessarily state or reflect those of the United States Government or any agency thereof.

DISCLAIMER

Portions of this document may be illegible in electronic image products. Images are produced from the best available original document.

MECHANICAL PROPERTIES OF $\text{Ce}_{0.9}\text{Gd}_{0.1}\text{O}_{2-x}$ AND $\text{Ce}_{0.9}\text{Gd}_{0.1}\text{O}_{2-x} + \text{Al}_2\text{O}_3$ COMPOSITES

J. L. Routbort and K. C. Goretta
Energy Technology Division
Argonne National Laboratory, Argonne, IL 60439

R. Doshi, V. L. Richards, and M. Krumpelt
Chemical Technology Division
Argonne National Laboratory, Argonne, IL 60439

J. Wolfenstine
Division of Engineering
University of Texas at San Antonio, San Antonio, TX 72849

and A. R. de Arellano-López
Department of Condensed Matter Physics
University of Sevilla, 41080 Sevilla, Spain

ABSTRACT

The room-temperature elastic moduli, fracture strength, and fracture toughness of dense, fine-grained, pure $\text{Ce}_{0.9}\text{Gd}_{0.1}\text{O}_{1.95}$ and composites containing 1.3 and 9.1 wt.% Al_2O_3 were investigated. Addition of 9.1 wt.% Al_2O_3 to $\text{Ce}_{0.9}\text{Gd}_{0.1}\text{O}_{1.95}$ changed the fracture mode from intergranular to transgranular and increased room-temperature fracture strength from 65 to 125 MPa and fracture toughness from 1.3 to 1.6 $\text{MPa m}^{1/2}$. In addition, steady-state compressive creep was measured for $\text{Ce}_{0.9}\text{Gd}_{0.1}\text{O}_{1.95}$ and the $\text{Ce}_{0.9}\text{Gd}_{0.1}\text{O}_{2-x} + 9.1$ wt.% Al_2O_3 composite. The stress exponent ≈ 1.3 and the activation energy ≈ 480 kJ/mole for $\text{Ce}_{0.9}\text{Gd}_{0.1}\text{O}_{1.95}$ suggested diffusional flow controlled by the cations. There was no difference in creep rate between $\text{Ce}_{0.9}\text{Gd}_{0.1}\text{O}_{2-x}$ and the composite.

INTRODUCTION

Ceria-based electrolytes have potential for use in intermediate-temperature solid oxide fuel cells (SOFCs) or double-layer electrolyte-based SOFCs [1-3]. Ceria-based fuel cells are currently being developed in several countries [4-6]. The reduced operating temperatures of these fuel cells, while having advantages of reduced startup time, increased thermal cycle ability, and use of metallic interconnects with reduced oxidation problems, require either a very thin form of a conventional zirconia electrolyte or a different electrolyte with higher ionic

conductivity. Cerium oxide electrolytes doped with rare earths such as gadolinium exhibit higher ionic conductivity in air than does zirconia [7].

Electrolytes must exhibit enough fracture strength, fracture toughness (K_{IC}), and creep resistance to survive the rigors of applications. Improved strength will allow ceria-based materials to be considered for SOFCs used in mobile energy sources. Increased toughness will improve the durability of the electrolyte and its ability to withstand thermal cycling. Higher creep resistance will improve dimensional stability at elevated temperatures if the electrolyte is under stress.

Very little is known about mechanical properties of these materials. Sammes and Zhang [8] reported that values of indentation K_{IC} of $Ce_{0.9}Gd_{0.1}O_{2-x}$ were in the range of 2.1 to 2.5 $MPa\text{m}^{1/2}$. The fracture strength has been reported to be 143 MPa [9]. Polycrystalline CeO_2 (94% theoretical density, TD) has a K_{IC} of 1.3 $MPa\text{m}^{1/2}$ and a strength of about 80 MPa [10]. Indentation and single-edge notched beam (SENB) fracture data were obtained on 94% TD $(CeO_2)_{0.9}(SmO_{1.5})_{0.1}$ and $(CeO_2)_{0.8}(SmO_{1.5})_{0.2}$. K_{IC} as measured by SENB ≈ 1.3 $MPa\text{m}^{1/2}$ for both compositions, but ≈ 2.4 $MPa\text{m}^{1/2}$ as measured by indentation techniques [11].

The objective of this work was to measure and compare the mechanical properties of $Ce_{0.9}Gd_{0.1}O_{2-x}$ and $Ce_{0.9}Gd_{0.1}O_{2-x} + Al_2O_3$ composites in order to ascertain if the addition of Al_2O_3 would produce a candidate electrolyte material that would be mechanically more robust than undoped $Ce_{0.9}Gd_{0.1}O_{2-x}$ and therefore be able to survive service applications.

EXPERIMENTAL DETAILS

The $Ce_{0.9}Gd_{0.1}O_{2-x}$ powder was obtained from Rhone Poulenc (France) with an average particle size of ≈ 1 μm and was cold-pressed into bars measuring approximately 38 x 6 x 3 mm at a pressure of 100 MPa. The pressed bars were sintered for 2 h at 1450°C in air to a final density of 92–96% TD. The grains after sintering were equiaxed and had a size of ≈ 1 μm . X-ray diffraction indicated that the $Ce_{0.9}Gd_{0.1}O_{2-x}$ was single-phase after sintering.

The $Ce_{0.9}Gd_{0.1}O_{2-x} + Al_2O_3$ composite materials were produced by mixing the $Ce_{0.9}Gd_{0.1}O_{2-x}$ powder with 1.33 or 9.1 wt.% 0.1- μm Al_2O_3 powder from Adolf Meller (Providence, RI). The powders were put into a solution of 60% H_2O and 40% isopropyl alcohol with ZrO_2 media. Before milling for 72–96 h, a dispersant (Darvan 821A, Vanderbilt, Norwalk, CT) and binders and plasticizers (15 wt.% polyvinyl alcohol in H_2O , glycerol, and PEG 400) were added to the solution. The pH was adjusted to ≈ 9 by adding NH_4OH . The well-mixed suspension was dried and the powder was ground with a mortar and pestle and sieved through a 100-mesh screen. The powders were pressed and fired as before, but care was taken to

slowly burn out the organics by heating at $1^{\circ}\text{C}/\text{min}$ to 400°C . The equiaxed average grain sizes of the composites were approximately equal to that of the pure material and are shown in Fig. 1A for the 9.1 wt.% composite. The Al_2O_3 distribution was best seen as dark areas in scanning electron microscopy (SEM) backscattered mode (Fig. 1B).

Fracture strength, σ_F , was measured in four-point bend tests at a crosshead velocity of $125\ \mu\text{m}/\text{min}$ on bars whose tensile surface had been ground with $3\text{-}\mu\text{m}$ diamond paste and whose edges were chamfered. The outer load span was 19 mm and the inner span was 9.5 mm. K_{IC} was measured by an SENB test with an outer span of 19 mm. The notch was between 0.2 and 0.4 of the width of the bar and was cut by a slow-speed diamond saw whose blade was $185\ \mu\text{m}$ thick. Data were analyzed by use of conventional formulae [12,13]. Elastic moduli were measured ultrasonically at 5 MHz. Microstructures were examined by SEM.

Samples with approximate dimensions of $3 \times 3 \times 6\ \text{mm}$ were cut from the bars. High-temperature compressive creep was measured at $1200\text{--}1300^{\circ}\text{C}$ in air for constant stress [14], crosshead velocity [15], or load [16] tests.

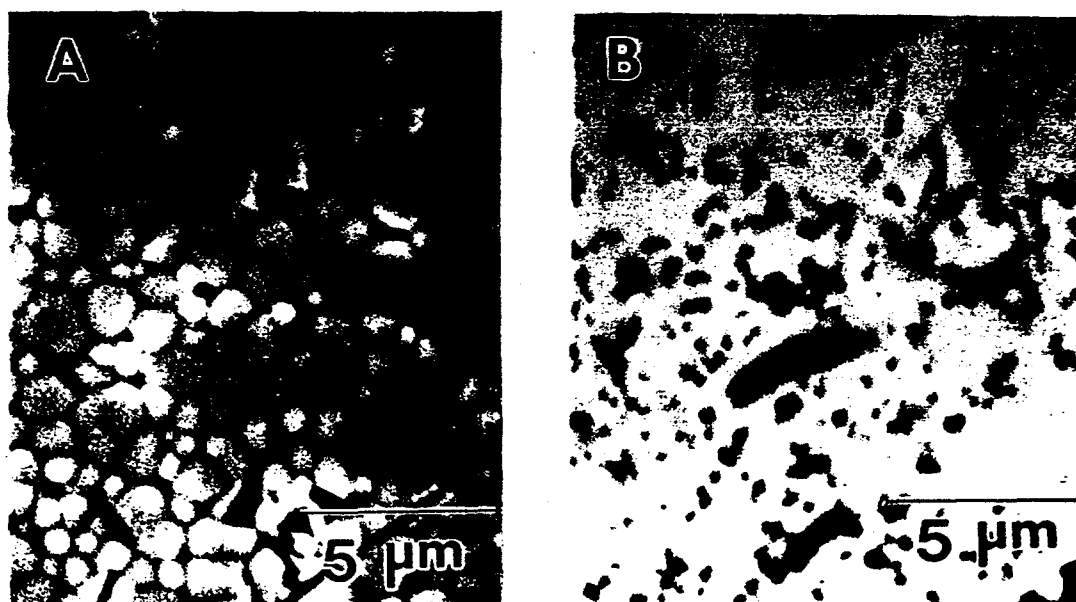


Fig. 1. SEM photomicrographs of thermally etched surface of $\text{Ce}_{0.9}\text{Gd}_{0.1}\text{O}_{2-x}$ + 9.1 wt.% Al_2O_3 obtained by (A) secondary mode and (B) backscattered mode. Dark areas are Al_2O_3 .

RESULTS AND DISCUSSION

A summary of the room-temperature mechanical properties is presented in Table 1. G is the shear modulus, E Young's modulus, and H_V Vickers hardness. H_V was independent of load and increased with increasing Al_2O_3 content. σ_F and K_{IC} of $Ce_{0.9}Gd_{0.1}O_{2-x}$ were about equal to values of similar materials cited in the Introduction. K_{IC} of $(CeO_2)_{0.9}(SmO_{1.5})_{0.1}$, as determined by SENB, was lower than that reported by indentation techniques, 1.3 compared to 2.1 to 2.5 $MPam^{1/2}$ [11].

K_{IC} measured by Vickers indentation [17] is shown in Fig. 2 as a function of load and compared with K_{IC} as measured by SENB. This behavior is rather like an inverse of R-curve behavior in that the toughness decreases as the crack length increases. This behavior is consistent with the results cited in Ref. 11. A possible explanation might be existence of residual stresses that would inhibit the growth of shorter cracks, but whose restraints would be removed as the cracks become longer. We have not explored this point.

Young's modulus for $Ce_{0.9}Gd_{0.1}O_{2-x}$ was somewhat higher than the 147 GPa reported for $Ce_{0.8}Gd_{0.2}O_{2-x}$ [10] (which is, however, lower than E for CeO_2). E for Al_2O_3 is more than a factor of 2 larger than E of CeO_2 . Therefore, it is surprising that the E of the Al_2O_3 composite is lower than that of the pure material. However, the composite was less dense ($\approx 91\%$ TD) and thus the difference could be partially the result of porosity. Hardness values were slightly lower than the values of 8.7 GPa reported for $(CeO_2)_{0.8}(SmO_{1.5})_{0.2}$ [11].

Table 1. Mechanical properties of $Ce_{0.9}Gd_{0.1}O_{2-x}$ and Al_2O_3 composites.

Material	G (GPa)	E (GPa)	H_V (GPa)	K_{IC} ($MPam^{1/2}$)	σ_F (MPa)
$Ce_{0.9}Gd_{0.1}O_{2-x}$	76 ± 2.0	204 ± 5.0	6.2 ± 0.4	1.30 ± 0.08	65.7 ± 16.4
$Ce_{0.9}Gd_{0.1}O_{2-x}$ + 1.33 wt.% Al_2O_3	—	—	7.1 ± 0.2	1.33 ± 0.11	64.9 ± 10.9
$Ce_{0.9}Gd_{0.1}O_{2-x}$ + 9.1 wt.% Al_2O_3	73 ± 1.0	184 ± 2.0	7.3 ± 0.5	1.60 ± 0.14	127.8 ± 11.1

The fracture strength of the 9.1 wt.% Al_2O_3 composite was improved by $\approx 100\%$, while K_{IC} was increased by $\approx 25\%$. A fracture surface of $Ce_{0.9}Gd_{0.1}O_{2-x}$ is shown in Fig. 3A. The fracture was mainly intergranular, although there were some instances of transgranular fracture. No specific critical flaw that would control the fracture strength was identified by SEM. The fracture mode indicated that the grain boundaries of the $Ce_{0.9}Gd_{0.1}O_{2-x}$ samples were relatively weak.

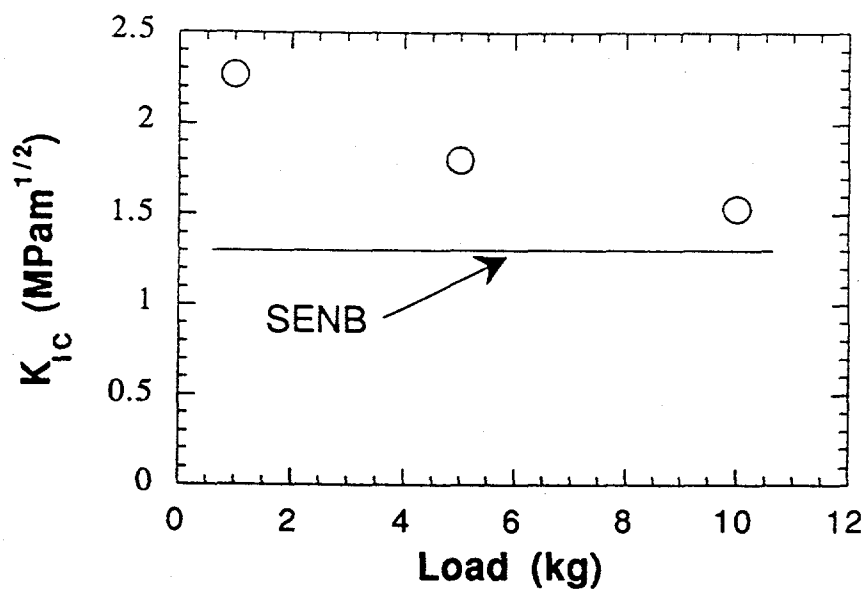


Fig. 2. Comparison of K_{IC} measured by Vickers indentations (points) with that measured by SENB on a $Ce_{0.9}Gd_{0.1}O_{2-x} + 1.33$ wt.% Al_2O_3 composite (straight line).

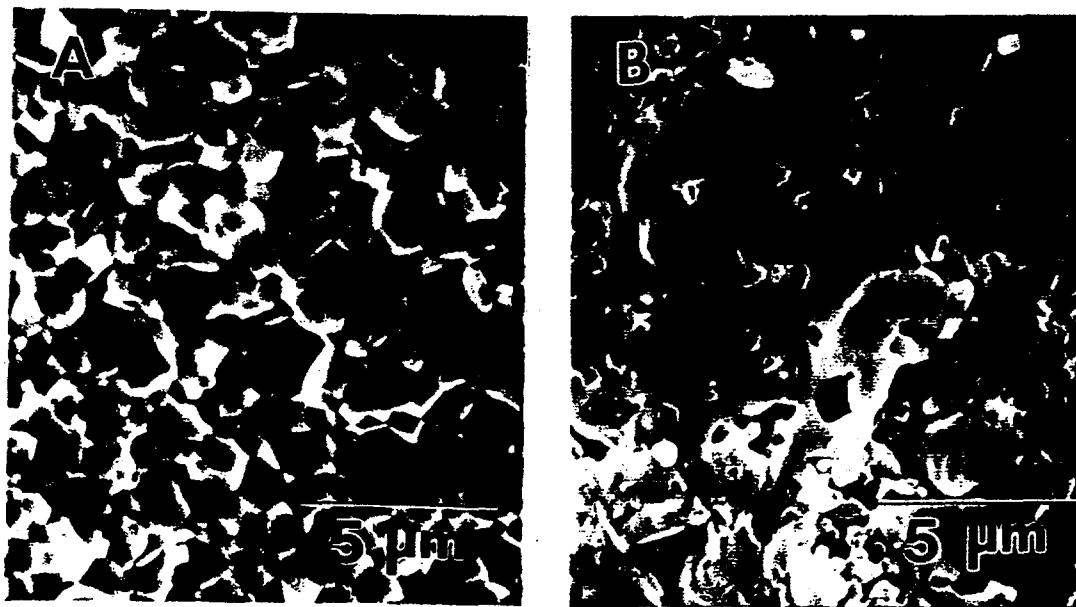


Fig. 3. SEM photomicrograph of fracture surface of (A) $Ce_{0.9}Gd_{0.1}O_{2-x}$ and (B) $Ce_{0.9}Gd_{0.1}O_{2-x} + 9.1$ wt.% Al_2O_3 .

The 9.1 wt.% composite, on the other hand, fractured primarily via a transgranular mechanism (Fig. 3B). Figures 1B and 3B show that the visible percentage of Al_2O_3 was lower than the 20.5 vol.% added. This indicates that some of the Al_2O_3 probably formed a solid solution with the $\text{Ce}_{0.9}\text{Gd}_{0.1}\text{O}_{2-x}$. The increases in σ_F , K_{IC} , and change of fracture mode may be the result of alloying. Al_2O_3 when dissolved into $\text{Ce}_{0.9}\text{Gd}_{0.1}\text{O}_{2-x}$ could act as a sintering aid that produces a ceramic with smaller critical flaws, thereby increasing σ_F . K_{IC} may increase because some of the Al_2O_3 segregates along the grain boundaries, which could increase the strength and change the fracture mode from intergranular to transgranular with the addition of Al_2O_3 . The K_{IC} of the 9.1 wt.% composite is about equal to that of $\text{Zr}_{0.92}\text{Y}_{0.08}\text{O}_{2-x}$ [18].

A full paper on the $\text{Ce}_{0.9}\text{Gd}_{0.1}\text{O}_{1.95}$ creep results is in press [19], but the principal results are summarized and compared to those of the composite here. Figure 4 presents a plot of the steady-state strain rate measured under conditions of constant crosshead velocity, load, and stress at 1300°C in air for $\text{Ce}_{0.9}\text{Gd}_{0.1}\text{O}_{1.95}$ and the 9.1 wt.% Al_2O_3 composite. The agreement between the three types of tests performed on $\text{Ce}_{0.9}\text{Gd}_{0.1}\text{O}_{1.95}$ in three different laboratories is gratifying and is further verification that the steady-state creep is established. That is, a unique relationship exists between the steady-state creep rate, $\dot{\epsilon}$, and the steady-state stress, σ_s .

The creep data for $\text{Ce}_{0.9}\text{Gd}_{0.1}\text{O}_{1.95}$ were described by the equation

$$\dot{\epsilon} \propto \sigma_s^{1.3 \pm 0.2} \exp[-(480 \pm 100 \text{ (kJ/mole)}/RT)],$$

where RT has its usual meaning. The phenomenological creep equation is valid from 1200 to 1300°C with stresses of 2–60 MPa. Strains >25% were obtained at 1300°C without fracture.

The above equation with its stress exponent close to unity strongly suggests that creep deformation is controlled by diffusional flow with an activation energy of 480 kJ/mole. The activation energy for oxygen diffusion in air, as measured by the isotope-exchange method, was reported to be 104 ± 15 kJ/mole [20], considerably lower than the creep activation energy of 480 kJ/mole. Additionally, $\text{Ce}_{0.9}\text{Gd}_{0.1}\text{O}_{1.95}$ is a fast oxygen conductor that results from very high vacancy concentration. Therefore, one might speculate that the diffusion of the cation Ce controls creep deformation. The activation energy for cation diffusion would involve the sum of a formation and a migration energy while that for anion diffusion does not involve a formation term because the oxygen vacancy is fixed by the Ce/Gd ratio. Figure 4 also reveals that the stress exponent for the 9.1 wt.% Al_2O_3 composite is close to unity, which implies that creep of the composite is also controlled by diffusional flow. In addition, it is observed that the creep resistance of this composite is similar to that of $\text{Ce}_{0.9}\text{Gd}_{0.1}\text{O}_{1.95}$; this is expected because the grain sizes of the two materials are similar.

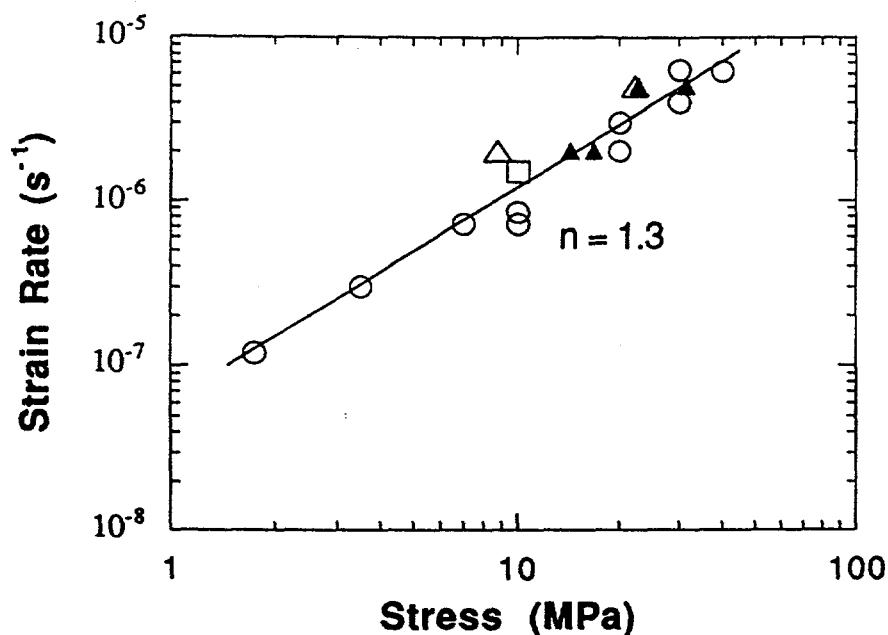


Fig. 4. Steady-state creep rate vs. stress for $\text{Ce}_{0.9}\text{Gd}_{0.1}\text{O}_{2-x}$ at 1300°C in air measured at constant load (circles), constant crosshead velocity (triangles), and constant stress (square). Data for 9.1 wt.% composite are also shown (filled triangles).

The creep resistance of $\text{Ce}_{0.9}\text{Gd}_{0.1}\text{O}_{2-x}$ at 1300°C and 10 MPa is about one order of magnitude lower than that extrapolated for a fine-grained $\text{Zr}_{0.6}\text{Y}_{0.4}\text{O}_{1.8}$ ceramic [21], but is still quite good.

SUMMARY

The addition of 9.1 wt.% Al_2O_3 to $\text{Ce}_{0.9}\text{Gd}_{0.1}\text{O}_{2-x}$ improves the strength and toughness such that the resultant mechanical properties are competitive with those of $\text{Zr}_{0.92}\text{Y}_{0.08}\text{O}_{2-x}$, which is the current electrolyte material under consideration for a solid oxide fuel cell. The elastic moduli and Vickers hardness for the pure and 1.3 and 9.1 wt.% Al_2O_3 composites are comparable to those measured for similar ceramics. K_{IC} determined by indentation techniques is higher than K_{IC} measured by SENB, but the values approach each other for long crack lengths. High-temperature compressive creep has been measured at 1200–1300°C, and the results indicate that creep deformation is controlled by diffusional flow of the cation with an activation energy of ≈ 480 kJ/mole. Addition of Al_2O_3 does not affect the creep rate. The creep rate of $\text{Ce}_{0.9}\text{Gd}_{0.1}\text{O}_{1.95}$ is about one order of magnitude higher than that for $\text{Zr}_{0.6}\text{Y}_{0.4}\text{O}_{1.8}$.

Acknowledgments

We are grateful to M. Burdt, M. Cuber, M. Sutaria, and N. Vasanthamohan for assistance with the experiments. This work was supported by the U.S. Department of Energy under Contract W-31-109-Eng-38, and by the Ministerio de Educación y Ciencias of Spain, under CICYT Project MAT94-0481.

References

1. K. Eguchi, T. Setoguchi, T. Inoue, and H. Arai, *Sol. St. Ion.* **52**, 165 (1995).
2. D. L. Maricle, T. E. Swarr, and S. Karavolis, *Sol. St. Ion.* **52**, 173 (1995).
3. M. Mogensen, T. Lindegaard, and U. R. Hansen, *J. Electrochem. Soc.* **141**, 2122 (1994).
4. M. Sahibzada, et al., *Proc. 2nd European Solid Oxide Fuel Cell Forum*, Oslo, Norway, ed. B. Thorstenen, Vol. 2, p. 687.
5. B. C. H. Steele, K. Zheng, N. Kiratzis, R. Rudkin, and G. M. Christe, *Proc. Fuel Cell Seminar*, San Diego, CA, Nov. 1994, p. 479.
6. C. Milliken, S. Elangovan, J. Hartvigsen, and A. Khandkar, *EPRI/GRI Fuel Cell Workshop*, Tempe, AZ, Apr. 2-3, 1996.
7. R. Doshi, J. Routbort, and M. Krumpelt, *Fuel Cell Seminar*, Kissimmee, FL, Nov. 17-20, 1996.
8. N. M. Sammes and Y. Zhang, *Proc. 2nd European Solid Oxide Fuel Cell Forum*, Oslo, Norway, ed. B. Thorstenen, Vol. 2, p. 697.
9. N. Sammes, G. Tompsett, Y. Zhang, A. Cartner, and R. Torrens, *Denki Kagaku* **64**, 674 (1996).
10. S. Maschio, O. Sbaizero, and S. Meriani, *J. Euro. Ceram. Soc.* **9**, 127 (1992).
11. J. E. Shemilt, H. M. Williams, M. J. Edirisinghe, J. R. G. Evans, and B. Ralph, *Scripta Mater.* **36**, 929 (1997).
12. ASTM C1161 (1990), "Standards for Measuring of Bending Strength of Structural Ceramics".
13. ASTM E399-90 (1990), "Standard Test Method for Plain-Strain Fracture Toughness of Metallic Materials".
14. H. Duong and J. Wolfenstine, *Phys. Stat. Sol. A* **129**, 379 (1992).
15. J. Routbort, *Acta Metall.* **30**, 663 (1982).
16. H. Gervais, B. Pellissier, and J. Castaing, *Rev. Int. Hautes Temp. Refract.* **15**, 43 (1978).
17. A. G. Evans and E. A. Charles, *J. Am. Ceram. Soc.* **59**, 371 (1976).
18. J. P. Singh, A. L. Bosak, C. C. McPheeters, and D. Dees, *Proc. Fuel Cell Seminars*, Long Beach, CA, Oct. 23-26, 1988, p. 145.
19. J. L. Routbort, K. C. Goretta, A. R. de Arellano-López, and J. Wolfenstine, *Scripta Mater.*, in press (1998).
20. R. Freer, *J. Mater. Sci.* **15**, 803 (1980).
21. D. Dimos and D. L. Kohlstedt, *J. Am. Ceram. Soc.* **70**, 531 (1987).